ABSOLUTE Nuv MAGNITUDES OF GAIA DR1 ASTROMETRIC STARS AND A SEARCH FOR HOT COMPANIONS IN NEARBY SYSTEMS

Valeri V. Makarov

US Naval Observatory, 3450 Massachusetts Ave NW, Washington DC 20392-5420, USA

ABSTRACT

Accurate parallaxes from Gaia DR1 (TGAS) are combined with GALEX visual Nuv magnitudes to produce absolute Mnuv magnitudes and an ultraviolet HR diagram for a large sample of astrometric stars. A functional fit is derived of the lower envelope main sequence of the nearest 1403 stars (distance < 40 pc), which should be reddening-free. Using this empirical fit, 50 nearby stars are selected with significant Nuv excess. These are predominantly late K and early M dwarfs, often associated with X-ray sources, and showing other manifestations of magnetic activity. The sample may include systems with hidden white dwarfs, stars younger than the Pleiades, or, most likely, tight interacting binaries of the BY Dra-type. A separate collection of 40 stars with precise trigonometric parallaxes and Nuv−G colors bluer than 2 mag is presented. It includes several known novae, white dwarfs, and binaries with hot subdwarf (sdOB) components, but most remain unexplored.

RESUMEN

Se combinan paralajes del Gaia DR1 (TGAS) con magnitudes visuales Nuv del GALEX para obtener magnitudes absolutas Mnuv así como un diagrama HR ultravioleta para una muestra de estrellas astrométricas. Se deriva un ajuste para la envolvente inferior de la secuencia principal para las 1403 estrellas con distancias < 40 pc, que no tendrían enrojecimiento. Se seleccionan 50 estrellas cercanas con un exceso Nuv considerable. Estas estrellas son principalmente de tipo K tardío y M temprano, frecuentemente asociadas con fuentes de rayos X, y con otras manifestaciones de actividad magnética. La muestra puede incluir sistemas con enanas blancas ocultas, estrellas más jóvenes que las Pléyades o binarias interactuantes de tipo BY Dra. Se presenta otra muestra de 40 estrellas con paralajes trigonométricas precisas y colores Nuv-G más azules que 2 mag. Ésta incluye varias novas, enanas blancas y binarias con subenanas calientes como compañeras.

Key Words: binaries: general — Hertzsprung–Russell and C–M diagrams — stars: activity — white dwarfs

1. INTRODUCTION

The first release of the Gaia mission data (Gaia DR1) includes two astrometric catalogs (Brown and Gaia Collaboration 2016). The smaller catalog, called TGAS, includes 2 million brighter stars with accurate proper motions and parallaxes and is based on a combination of astrometric data from Hipparcos and Tycho-2 (ESA 1997; Høg et al. 2000) and Gaia itself (Lindegren et al. 2016), while the larger catalog of 1.1 billion objects is derived from Gaia's own observations and ICRF-2 radio source positions. I am using the TGAS in this paper, specifically, the parallaxes of brighter stars listed there. The formal errors of parallaxes are all smaller than 1 mas, which was the only requirement for an astrometric solution to be included in DR1. The entire set of 2 million Gaia DR1 stars was cross-matched with the GALEX DR5 catalogs by Bianchi et al. (2011), namely, the All-Sky Imaging survey (AIS) with limiting magnitudes 19.9/20.8 in FUV/NUV and the Medium-depth Imaging Survey (MIS) with limiting magnitudes 22.6/22.7. The search for Galex matches was performed with Gaia J2015 positions in a cone of 3.5σ of Galex positions, but not greater than $5''$

on the sky. The total number of matched sources is
720 622, which is a surprisingly high rate given that
the GALEX catalog covers only a little more than
half of the sky[1]. GALEX DR5 provides precise far-
ultraviolet (Fuv; 1344-1786 Å) and near-ultraviolet
(Nuv; 1771-2831 Å) magnitudes with errors gener-
ally about 0.02–0.03 mag. We thus obtain a large
collection of astrometric standards with good par-
allaxes and UV magnitudes which can be used to
compute *absolute* ultraviolet magnitudes:

$$M\text{nuv} = \text{Nuv} - 10 + 5\log\varpi, \qquad (1)$$

where ϖ is the parallax in mas. The uncertainty
of absolute magnitudes is dominated by the error of
Nuv magnitude for most of the stars, but distant
objects (small parallaxes) can have the ratio ϖ/σ_ϖ
close to unity, to the point that the observed par-
allax takes a negative value. To reduce the astro-
metric noise component in the subsequent analysis,
the sample needs to be limited to the most reliable
determinations with large ϖ/σ_ϖ or, which is almost
equivalent in this case, with large parallaxes.

2. THE HERTZSPRUNG–RUSSELL DIAGRAM IN THE NEAR-ULTRAVIOLET

Figure 1 displays the "absolute Nuv magnitude
versus Nuv−G color" (HR) diagram for 1403 stars
selected with the logical *and*, or intersection, of the
following criteria: $\varpi/\sigma_\varpi > 5$; $\varpi > 25$ mas. Al-
though observed B_T and V_T magnitudes are avail-
able for all Tycho-2 stars, as well as derived Johnson
B and V magnitudes, I will use the more accurate
broadband G magnitudes as observed by Gaia. For
the sample under consideration, the distribution of
formal errors of G magnitudes peaks at 0.0005 mag
with a median of 0.0009 mag. This is much smaller
than the uncertainty of Nuv magnitudes. The selec-
tion includes stars confidently within 40 pc of the
Sun.

Most of the stars lie on a well-defined and nar-
row main sequence stretching between magnitudes 9
and 22 in absolute magnitude Mnuv and 5 – 12 in
Nuv−G color. There is a rudimentary giant branch
veering off to the right at the top of the main se-
quence, reflecting the scarcity of giants in the im-
mediate solar neighborhood. The width of the main
sequence is roughly 0.5 mag, likely to come from un-
resolved binaries. A regular MS–MS binary is shifted
up and to the right of the main sequence because
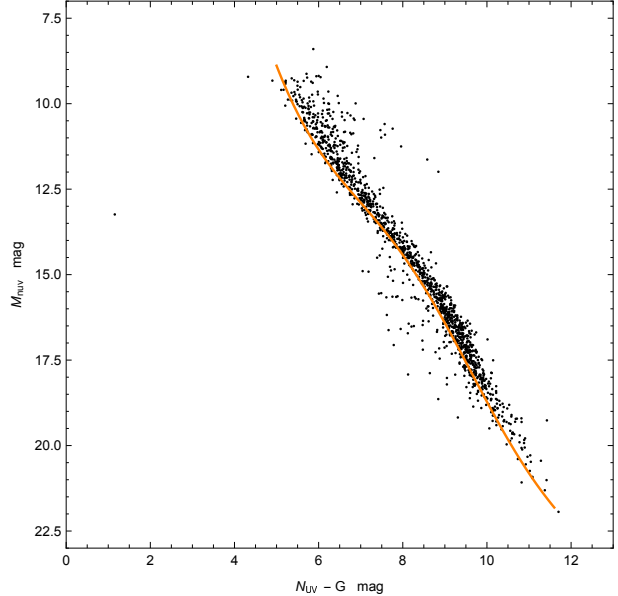there is more additional flux in the G band than

---

[1] There is a wide empty swath in GALEX along the Galac-
tic plane due to the source confusion.

Fig. 1. Near-UV HR diagram of absolute Nuv magni-
tudes versus Nuv−G colors for nearby stars with par-
allaxes greater than 25 mas, matched with GALEX
sources. The single dot far to the left represents the
only single white dwarf in the sample, DN Dra. The line
along the lower envelope of the main sequence shows the
formal functional fit, see text.

in Nuv. The largest deviation from the main se-
quence due to binarity is ≈ 0.75 mag for identical
twin pairs. Interstellar reddening is not expected to
have a significant presence in this diagram as there
are no dense dust-molecular clouds within 40 pc.

Using a standard nonlinear fit algorithm (min-
imizing the residual RMS), this functional form is
found for the *lower envelope* main sequence, repre-
sented with a solid curved line in Figure 1:

$$\begin{aligned}M\text{nuv(fit)} &= 15.339 + 5.708\,x - 1.653\,x^2 + \\ &\quad 1.029\,x^3 - 0.915\,\cos[\pi x], \qquad (2)\end{aligned}$$

where $x = (\text{Nuv} - G - 8)/3.3$. This curve accurately
represents the bluest magnitudes and colors of nor-
mal field dwarfs without any signs of activity or red-
dening. The presence of a cosine term is justified by
the much better results achieved: the standard devi-
ation of post-fit residuals over a set of nodal points
goes down from 0.21 to 0.08 mag, and the observed
wiggles of the lower envelope are much more truth-
fully represented. A median main sequence func-
tional expansion can be obtained from Equation 2
by replacing the constant term 15.339 with 15.150.

The inverse main sequence fit, i.e., [Nuv − G](Mnuv) may be handy if we want to estimate the amount of observed "UV-excess" for a known absolute magnitude:

$$[\mathrm{Nuv} - G](\mathrm{fit}) = 8.096 + 3.463\,y + 0.786\,y^2 -$$
$$0.120\,y^3 + 0.482\,\cos[\pi y], \quad (3)$$

where $y = (M\mathrm{nuv} - 15.5)/6.5$.

A few dozen stars lie to the left of the lower boundary curve with either their colors too blue or absolute magnitudes too faint. The latter is unlikely because of the slope of the main sequence – a deficit of Nuv flux would shift the point to the right of the main sequence. Hence, the stars below and to the left of the main sequence envelope have ultraviolet excess with respect to normal luminosities. This is confirmed by Figure 2 which shows a similar HR diagram for the same set of stars, but with Fuv magnitudes instead of Nuv. The main sequence is not well defined in the far-UV, but the stars with a large Nuv luminosity excess occupy a specific area of the diagram with absolute Fuv magnitudes greater than 6.7 and Fuv−G colors less than 11.6. This confirms that the ultraviolet excess for a fraction of nearest dwarfs is real and present in a wide range of wavelengths.

3. NEARBY STARS WITH NUV EXCESS

Table 1 lists nearby stars (distance less than 40 pc) found in the TGAS–GALEX sample with significant Nuv luminosity excess. The latter was defined as $M\mathrm{Nuv(obs)} - M\mathrm{Nuv(fit)} > 0.7$ mag. This is a conservative limit possibly leaving out a number of genuine sources of enhanced UV radiation, but it results in a more manageable sample of 50 stars which can be individually verified. The columns of the table include: (1) RA J2015 in degrees; (2) Dec J2015 in degrees; (3) HIP number when available; (4) Tycho-2 identification when HIP number is not available; (5) parallax in mas; (6) standard error of parallax in mas; (7) G magnitude; (8) Fuv magnitude, if available; (9) Nuv magnitude; (10) formal error of Fuv magnitude, if available; (11) formal error of Nuv magnitude. Columns 1 through 7 are copied from TGAS, while Columns 8 – 11 are copied from GALEX.

The single point far to the left in Figures 1 and 2 represents the well-known white dwarf **DN Dra = GJ 1206** of spectral type DA4.0 (e.g., Fontaine et al. 1992). It is very luminous in the near-UV with an absolute magnitude $M\mathrm{nuv}= 7.95$ mag. The absence of other bright white dwarfs within 40 pc of the Sun
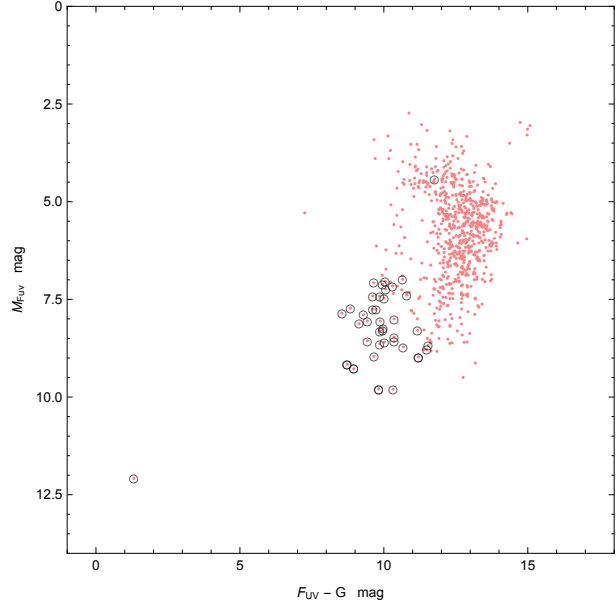

Fig. 2. Far-UV HR diagram of absolute Fuv magnitudes versus Fuv−G colors for nearby stars with parallaxes greater than 25 mas, matched with GALEX sources. The single encircled dot in the lower left corner represents the only single white dwarf in the sample, DN Dra. Stars of significant Nuv luminosity excess collected in Table 1 are also marked with circles.

in our selection is probably explained by selection effects in the Hipparcos, Tycho-2, and TGAS catalogs[2]. Other excess stars have much redder Nuv−G colors and cannot be isolated white dwarfs. An extensive literature and astronomical database search with VizieR and Simbad reveals that the sample includes predominantly dwarfs of late K to early M spectral types. Some of these stars are included in the study of the near-UV luminosity function of early M-type dwarfs by Ansdell et al. (2015), where the authors used Nuv fluxes relative to visual and near-infrared fluxes rather than absolute luminosities, which leads to a larger sample. Ansdell et al. (2015) find that up to 1/6 of all such M dwarfs show elevated levels of near-UV radiation, which may be inconsistent with a constant star-formation rate and commonly used age-activity relations. Here we find a much lower rate of dwarfs with excess Nuv lumi-

---

[2]Gontcharov et al. (2011) find only 15 WD from Hipparcos and Tycho-2 using their astrometric and photometric criteria, but only 4 of them are present in TGAS with listed parallaxes and proper motions, namely, HIP 82257 = DN Dra, TYC 3953-480-1 = Eggr 378, TYC 8942-2593-1, and TYC 1538-1368-1, the latter two being false positives (not WD) because of gross errors in the Tycho-2 proper motions. The cause of this low representation rate is unknown.

TABLE 1

NEARBY DWARFS (DISTANCE < 40 PC) WITH EXCESS Nuv LUMINOSITY

(1)	(2)	(3)	(4)	(5)	(6)	(7)	(8)	(9)	(10)	(11)
RA J2015	Dec J2015	HIP	Tycho-2	ϖ	σ_ϖ	G	Fuv	Nuv	Fuv sig	Nuv sig
deg	deg			mas	mas	mag	mag	mag	mag	mag
51.028	23.7845	15844		48.59	0.31	9.809	19.779	18.072	0.206	0.053
35.8615	22.7347	11152		36.86	0.34	10.291	19.432	17.723	0.152	0.041
37.4013	34.3948		2331-1138-1	26.29	0.91	11.46	20.888	19.081	0.298	0.079
10.7024	35.5491	3362		46.4	0.31	9.422	19.032	17.411	0.141	0.027
15.9179	40.8574	4967		30.33	0.52	10.008	19.864	17.654	0.192	0.043
168.974	55.3304		3828-36-1	35.03	0.29	10.332	20.206	17.82	0.239	0.029
169.016	52.7767	55043		25.69	0.25	7.842		12.165		0.003
158.462	49.1867	51700		26.44	0.28	7.313	19.071	12.214	0.111	0.003
97.7541	50.046		3384-35-1	49.58	0.24	10.119	20.14	18.239	0.163	0.032
108.118	45.4218		3392-2038-1	25.19	0.33	10.802		18.646		0.063
139.843	62.0531	45731		25.75	0.38	10.359	19.974	18.127	0.112	0.02
149.623	67.054	48899		33.47	0.29	9.769	20.563	18.078	0.218	0.023
159.943	65.7559		4150-1189-1	30.77	0.38	10.561	20.916	19.033	0.315	0.076
94.5296	75.1012		4525-194-1	32.23	0.42	10.35	19.641	18.104	0.115	0.033
230.471	20.9783	75187		86.81	0.38	8.948	18.809	16.897	0.084	0.019
233.155	46.8846		3483-856-1	38.11	0.7	10.559	20.912	19.025	0.205	0.066
252.108	59.0551	82257		91.04	0.5	12.288	13.606	13.443	0.007	0.004
332.877	18.4269	109555		85.75	0.3	9.112	20.599	18.624	0.228	0.06
274.354	48.3675		3529-1437-1	50.28	0.88	10.211	20.884	18.688	0.278	0.062
279.857	69.0518		4430-329-1	30.79	0.47	10.871	20.733	19.078	0.231	0.068
5.03554	-17.0614	1608		43.31	0.57	11.687		20.996		0.216
347.082	-15.41	114252		39.85	0.25	10.052	19.482	17.662	0.109	0.03
347.168	-16.3833		6395-1046-1	26.15	0.61	9.899	20.549	17.351	0.376	0.053
339.692	-20.6215	111802		112.68	0.38	8.035	17.996	16.175	0.051	0.014
353.129	-12.2646		5832-666-1	36.02	0.53	9.684	19.692	17.89	0.119	0.034
2.77028	-5.78394	897		41.88	0.91	11.129		19.772		0.06
340.293	-16.4196		6386-326-1	25.01	0.98	11.501		20.279		0.168
73.1023	-16.8236		5899-26-1	63.4	0.37	10.264	19.219	18.049	0.109	0.039
72.491	-14.2861		5328-261-1	27.87	0.32	10.527		19.141		0.072
110.931	20.4153		1355-214-1	36.12	0.31	9.369	19.668	17.089	0.139	0.028
203.679	-8.34242	66252		48.39	0.35	8.614	18.659	16.42	0.114	0.023
165.66	21.9669	53985		83.77	0.35	8.678	19.848	17.543	0.204	0.038
230.356	4.24718		344-504-1	36.44	0.84	10.872	22.411	20.118	0.453	0.107
259.975	26.5023	84794		93.18	0.49	9.951	20.271	18.794	0.197	0.063
38.5944	-43.7976	11964		86.14	0.32	8.052	16.892	15.238	0.03	0.009
0.614199	-46.0289	191		27.17	0.39	11.409	21.76	20.286	0.393	0.09
47.0292	-24.7591	14568		30.74	0.4	9.635	19.282	17.331	0.125	0.035
28.2985	-21.0951		5858-1893-1	31.85	0.6	10.336	18.88	17.382	0.086	0.03
25.8094	-21.6157	8038		32.35	0.85	9.566	19.518	16.956	0.101	0.016
45.6603	-18.1656	14165		52.47	0.31	10.586		20.261		0.107

TABLE 1 (CONTINUED)

(1)	(2)	(3)	(4)	(5)	(6)	(7)	(8)	(9)	(10)	(11)
RA J2015	Dec J2015	HIP	Tycho-2	ϖ	σ_ϖ	G	Fuv	Nuv	Fuv sig	Nuv sig
deg	deg			mas	mas	mag	mag	mag	mag	mag
117.301	-76.7027		9381-1809-1	92.06	0.49	9.975	19.797	18.101	0.15	0.035
130.385	-68.4272	42650		32.84	0.52	10.289		18.771		0.081
159.939	-44.5109		7722-1583-1	53.57	0.97	10.519	19.247	19.567	0.148	0.121
161.298	-26.1259		6638-293-1	30.3	0.6	9.965		18.249		0.038
139.085	-18.6252		6032-282-1	73.35	0.94	9.647	20.844	18.696	0.319	0.097
201.451	-28.3744	65520		65.	0.31	9.957		19.55		0.114
349.888	-39.6569		8006-520-1	25.59	0.77	11.103		20.095		0.105
341.242	-33.251	112312		48.17	0.57	10.547	20.203	18.209	0.142	0.036
311.291	-31.3424	102409		102.12	0.39	7.712	17.442	15.588	0.042	0.01
318.272	-17.4875		6351-286-1	26.91	0.53	10.087	20.148	18.092	0.171	0.035

nosities in absolute units ($\sim 3.6\%$). It is possible that a relative-flux selection is biased toward more active M dwarfs from a larger volume of space.

3.1. Too Many Young Stars?

All of our late-type dwarfs satisfy the rather generous selection criteria for young stars of Rodriguez et al. (2013, their Fig. 1). Can they all be young? Assuming a constant rate of star formation over the 13 Gyr history of the Galaxy, the rate of overluminous dwarfs corresponds to a threshold age of 460 Myr. Hence, the existence of such dwarfs in the solar neighborhood can be explained if stars younger than the Hyades can retain the observed Nuv excess due to a high level of magnetic activity fueled by fast rotation. There are no star forming regions, OB associations, or young open clusters within the close solar neighborhood. However, some of the stars listed in Table 1 have been proposed as members of sparse young moving groups (YMG). Some interesting examples are:

- **TYC 5899-26-1**, an M3.3 dwarf, was assigned by Shkolnik et al. (2012) to the AB Doradus YMG with an estimated age of 30–50 Myr (Makarov 2007).

- **TYC 5832-666-1**, a rotationally variable M0 dwarf, was assigned by Lépine & Simon (2009) to the β Pic YMG with an estimated age of 20–30 Myr.

- **HIP 84794 = GJ 669A**, a flaring M3.5 dwarf, was assigned by Shkolnik et al. (2012) to the Hyades MG with an estimated age of 600 Myr[3].

- **HIP 112312 = WW PsA**, an M1 dwarf, was assigned by Shkolnik et al. (2012) to the β Pic MG, but it is also a rotationally variable binary of the BY Dra type.

- **HIP 102409 = GJ 803 = AU Mic**, a famous M1e young dwarf with a resolved debris disk, considered to be a member of the β Pic MG, but also an active binary of the BY Dra type.

- **TYC 6351-286-1 = HD 201919**, a rotationally variable K6Ve dwarf suggested by Elliott et al. (2016) as a member of the AB Doradus YMG.

Shkolnik & Barman (2014) conclude that the median UV flux of early M stars remains at "saturated" levels for a few hundred Myr, and the decline in activity after ≈ 300 Myr follows a time^{-1} dependence, but their analysis is based on rather rough distance estimates and the relative F_{UV}/F_J flux ratio. Often, the proposed membership of stars to the nearest moving groups is uncertain and suffers from considerable rates of interlopers. The earlier attempts at identifying such groups were based on proper motion and X-ray count rate data following the successful completion of the Rosat and Tycho-2 missions (Makarov & Urban 2000). But the census of nearby most luminous stars in X-rays shows that this criterion nets more active binaries of the

---

[3]The existence of the Hyades moving group as a coeval aggregate of stars has been disputed, (e.g., Famaey et al. 2007).

RS CVn and BY Dra type than very young objects (Makarov 2003). Even though the majority of objects in Table 1 are associated with Rosat-detected X-ray sources, this does not guarantee their young age. Figure 3 presents an attempt to verify that the over-luminous dwarfs can be younger than the Hyades. Only 9 known Pleiades members seem to be present in the TGAS–GALEX sample, marked with open circles. These stars are solar-type or earlier, and they conform to the main sequence fit quite well. Unfortunately, small-mass dwarfs are missing, perhaps because they are too faint. The filled circles represent the proposed members of the nearer and possibly younger Tuc Hor MG (estimated age 27 Myr) from Makarov (2007); Kraus et al. (2014). They allow us to probe later spectral types down to the early K. These candidate young stars start to deviate from the main sequence at Mnuv≈14–15 mag. This may be interpreted as a "turn-on" point of very young stars, which is likely age-dependent. The absence of late-type dwarfs thwarts verification of this result. The preliminary conclusion is that stars younger than the Pleiades ($\lesssim$ 100 Myr) that wandered by chance into the close solar neighborhood may be significantly over-luminous in the UV compared to older inactive field stars, but their number should be much smaller than what we find on the HR diagram.

3.2. *Hidden White Dwarfs*

The selection criteria adopted in § 3 are sensitive to unresolved binaries that include a cool main sequence dwarf and a hotter white dwarf (WD). Fuhrmann et al. (2016) speculated that binaries with WD companions should be quite common in the solar neighborhood but it is not easy to find them on account of their optical dimness. In principle, the near-UV HR diagram method should be capable of detecting hidden WD companions from the youngest and hottest (but rare) to objects as late as D8, or approximately 6300 K in effective temperature, but the prospects strongly depend on the spectral type of the main-sequence primary. The easiest and the most common target would be M dwarfs, and indeed, the prevalence of such objects in Table 1 can be explained this way. The dashed curved line in Fig. 3 shows the loci of M–WD pairs with completely blended photometry, where the cool nearby WD **van Maanen 2 = GJ 35 = HIP 3829** is used as a WD template. GJ 35 is a very close Population II white dwarf which is missing in TGAS (but present in the main Gaia catalog) of DZ7.5 spectral type, marked with a diamond on the diagram. Blended MS–WD
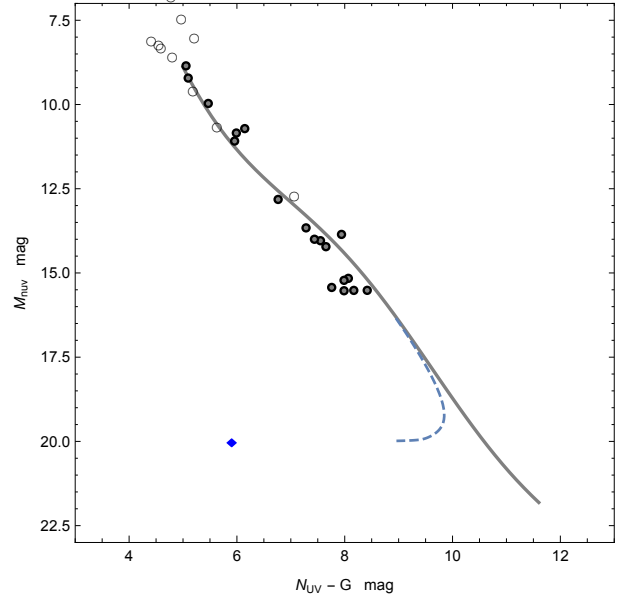

Fig. 3.— Near-UV HR diagram of absolute Nuv magnitudes versus Nuv−G colors for known members of the Pleiades cluster (open circles) and Tuc Hor MG members (filled disks) found in the TGAS–GALEX cross-match. The diamond in the lower left corner shows the data for the nearby white dwarf van Maanen 2. The solid line is the main sequence fit for nearby stars (Equation 2). The dashed line shows the computed loci of old inactive dwarfs in unresolved binaries with white dwarfs identical to van Maanen 2.

pairs cannot be bluer than the WD component or significantly redder than the MS component; thus, their positions are limited to the sharp angle formed by the main sequence and the horizontal line through the Mnuv of the WD. No WD companions have been identified in the literature for stars listed in Table 1 but their existence cannot be ruled out.

3.3. *Fast Rotation, Binarity, Flares*

Most of the stars with excess Nuv luminosity in Table 1 are associated with X-ray sources. This is a necessary but not sufficient sign of stellar youth as active close binaries also possess elevated coronal X-ray emission (Micela et al. 1997). The nearest (within 50 pc) and the brightest X-ray emitters are phenomenologically separated into a few categories (Makarov 2003) dominated by (1) RS CVn-type binaries (with evolved components); (2) BY Dra-type active binaries (with MS components); (3) young stars; (4) contact binaries of WU UMa type; (5) rapidly rotating single evolved stars. Short-period binaries feature strongly in this census with RS CVn pairs being the most luminous X-ray emitters of all

field non-degenerate stars. The fast rotation of components required to maintain high levels of chromospheric and coronal activity is fueled by the angular momentum transfer via tidal interactions (Hut 1980). The same mechanism relatively quickly circularizes tight orbits, but the presence of more distant, misaligned tertiary companions can be a source of excitation for the eccentricity of the inner pair via the Lidov-Kozai cycle (Eggelton et al. 1998). This probably explains the high rate of Rosat-detected sources associated with resolved doubles (Makarov 2002) – these may be the visual components of interacting hierarchical triple systems. A quarter of the sample have been detected as active binaries of BY Dra-type, often flaring and rotationally variable with structured photospheres. Some objects of note include:

- **TYC 2331-1138-1 = CK Tri** is a variable mistakenly classified as RS CVn-type, but it is definitely a nearby pair of dwarfs of the BY Dra-type.

- **HIP 3362 = FF And** is a BY Dra-type variable consisting of two twin M1V companions, also an astrometric binary with an orbital solution by Jancart et al. (2005) with an orbital period of 2.170 d. Chugainov (1971) posited that the properties of the light curve are best explained by a large, cool spot on the surface.

- **HIP 51700** is one of the two F stars in the sample (F8), and possibly a short-period variable (Koen & Eyer 2002).

- **HIP 45731 = GJ 3547** is a flare M1.0V star, which is a SB2 according to Shkolnik et al. (2010) with an orbital period less than 20 d.

- **HIP 111802 = GJ 867A = FK Aqr**, a well-studied quadruple system of chromospherically active flare dwarfs. The primary which is listed in Table 1 is a pair of twin dM1e stars (Herbig & Moorhead 1965) with a period of 4.08 d.

- **TYC 1355-214-1 = V429 Gem** is a K5Ve variable of BY Dra type, possibly including a brown dwarf companion (Hernán-Obispo et al. 2015).

- **HIP 14568 = GJ 3203 = AE For**, an eclipsing binary consisting of two K7Ve dwarfs with possibly a brown dwarf tertiary (Zasche et al. 2012).

- **TYC 5858-1893-1** is one of the less studied stars of M2Ve type, detected as SB2 with a rotational and orbital period of 2.9 d (Shkolnik et al. 2010).

4. A WIDER SELECTION OF UV-LUMINOUS STARS

A broader search for genuine hot stars in TGAS can be made if we drop the small distance criterion and consider the entire population with statistically precise parallaxes and matching GALEX sources. Table 2 lists 40 stars found with the following criteria: $\varpi/\sigma_\varpi > 5$, and Nuv$-G < 2$ mag. The format of this table is the same as Table 1. Besides the previously found DN Dra, this selection includes one additional well-known WD of DA0.8 type, **HIP 12031=FS Cet**. With $G = 12.177$ mag, Nuv=12.371 mag, Mnuv= 7.95 mag, this star marks the top of the WD cooling sequence in the HR diagram. Between FS Cet and van Maanen 2, the range of absolute Nuv magnitudes of white dwarfs is $\approx [8, 20]$ mag, and this should make the Nuv HR diagram a suitable proxy for the spectroscopic determination of type.

Most of the objects in Table 2 are relatively poorly studied stars that have remained under the radar of observers. It is only now with the combination of precise GALEX photometry and Gaia parallaxes that we begin to see them as very unusual objects. Several stars, on the contrary, have been studied in more detail, including:

- **TYC 2298-1538-1 = BG Tri** is a nova variable (Khruslov 2008; Kazarovets et al. 2011).

- **TYC 2807-1623-1 = RX And** is a famous dwarf nova (e.g., Kaitchuck et al. 1988).

- **TYC 5270-1692-1** has been previously recognized as a UV source owing to the observations with the TD1 satellite. It is a binary with a solar-type and a hot subdwarf components (sdO+G) (Berger & Fringant 1980).

- **HIP 86329** is another spectroscopically resolved solar-type – hot subdwarf binary (sdOB+F/G) (Berger & Fringant 1980).

- **TYC 6485-79-1** is a binary comprising a solar-type and a hot subdwarf components (sdOB+F) (O'Donoghue et al. 2013).

- **HIP 8435 = GJ 2026** is a solar-type – hot subdwarf binary (sdO7+F/G) (Greenstein 1974).

TABLE 2

GAIA STARS WITH SIGNIFICANT PARALLAXES AND Nuv$-G$ COLORS LESS THAN 2 MAG

(1) RA J2015 deg	(2) Dec J2015 deg	(3) HIP	(4) Tycho-2	(5) ϖ mas	(6) σ_ϖ mas	(7) G mag	(8) Fuv mag	(9) Nuv mag	(10) Fuv sig mag	(11) Nuv sig mag
57.3453	27.2266		$1808-902-1$	1.94	0.27	11.49	12.453	13.337	0.005	0.004
60.133	27.4278		$1821-1013-1$	2.43	0.3	11.425	12.827	13.321	0.005	0.004
26.1982	32.5499		$2298-1538-1$	2.79	0.43	11.871	12.505	13.146	0.005	0.004
16.1481	41.2993		$2807-1623-1$	5.41	0.55	13.128	13.489	13.859	0.009	0.007
143.672	30.561	46993		5.42	0.44	12.09	18.923	13.482	0.109	0.006
143.717	31.0274		$2494-805-1$	4.67	0.56	12.849	15.752	13.734	0.026	0.006
154.487	55.2755		$3818-1084-1$	1.68	0.26	11.656	11.903	12.634	0.004	0.004
111.785	26.9674		$1918-1313-1$	1.67	0.3	11.888	13.728	13.711	0.008	0.004
102.816	56.6469		$3774-18-1$	1.33	0.26	11.923	12.896	13.354	0.005	0.004
108.52	70.0716		$4364-1209-1$	4.93	0.29	12.061	12.178	12.991	0.005	0.004
107.051	78.0469		$4530-502-1$	1.35	0.23	12.052	12.719	13.075	0.004	0.004
246.563	23.0584		$2043-1081-1$	2.3	0.45	10.847	12.1	12.558	0.005	0.003
252.108	59.0551	82257		91.04	0.5	12.288	13.606	13.443	0.007	0.004
216.785	72.9638		$4416-1269-1$	2.04	0.33	11.126	11.737	12.195	0.003	0.002
350.178	38.1755		$3230-1262-1$	3.86	0.31	12.875	19.167	14.12	0.077	0.005
300.943	71.6068		$4454-1229-1$	3.23	0.3	10.434		12.039		0.002
13.0627	-10.6629		$5270-1692-1$	5.52	0.94	11.154		12.406		0.002
38.782	3.73248	12031		13.06	0.76	12.177		12.371		0.003
350.122	28.494		$2249-1134-1$	2.22	0.31	11.83	12.966	13.39	0.005	0.003
0.551579	32.9799		$2263-1340-1$	2.51	0.39	11.043	11.951	12.597	0.004	0.003
349.259	29.9058		$2248-1765-1$	1.91	0.36	11.962	13.966	13.869	0.006	0.004
80.3045	-24.7822		$6479-610-1$	1.73	0.28	11.283	12.949	12.67	0.005	0.003
65.4181	-6.01938		$4733-1261-1$	3.27	0.34	11.385		13.334		0.004
235.694	-7.72293		$5597-9-1$	1.61	0.29	11.74	13.454	13.601	0.006	0.004
246.831	12.5777		$967-861-1$	1.63	0.31	11.351	12.657	12.688	0.004	0.003
264.588	29.1466	86329		3.35	0.26	10.284	11.694	11.994	0.003	0.003
67.44	-50.5233		$8075-508-1$	2.68	0.25	11.758	18.242	13.599	0.094	0.006
75.8936	-28.4547		$6485-79-1$	1.66	0.28	12.249		12.812		0.004
27.1839	-26.6038	8435		2.96	0.33	12.22	11.985	13.112	0.004	0.004
159.874	-31.182		$7186-829-1$	1.91	0.3	12.15		13.751		0.007
98.9003	-62.6401	31481		2.45	0.44	12.348	12.906	13.351	0.004	0.003
95.8846	-37.8134		$7613-283-1$	2.2	0.28	11.203	12.529	13.006	0.004	0.003
294.23	-59.285		$8786-1818-1$	2.36	0.38	11.265	13.055	13.009	0.007	0.005
314.203	-45.4108		$8408-609-1$	1.63	0.31	12.314	12.532	12.925	0.006	0.002
349.927	-55.6115		$8834-986-1$	1.47	0.27	11.864	14.533	13.33	0.012	0.004
324.116	-45.6489		$8424-668-1$	8.2	0.3	13.304	22.525	15.158	0.405	0.009
325.129	-31.4509		$7487-82-2$	2.98	0.36	12.118	17.326	13.737	0.032	0.003
309.558	-39.9754		$7954-1134-1$	2.73	0.47	10.397	12.214	12.214	0.003	0.002
288.606	-42.8892		$7926-1427-1$	1.5	0.27	11.278	13.159	12.742	0.008	0.004
323.833	-30.517		$7474-402-1$	2.17	0.39	11.46	16.421	13.456	0.024	0.003

- **HIP 31481 = RR Pic** is a nova variable (Samus' et al. 2003), and one of the earliest UV detections (Gallagher & Holm 1974).

The appearance of known novae and spectroscopic binaries with hot subdwarfs implies that more hidden WD and sdOB can be discovered among the relatively nearby objects listed in Table 2. Follow-up spectroscopic and photometric observations are perhaps the best way to find the nature of their excessive UV luminosity.

5. CONCLUSIONS

This study of nearby astrometric standards from the Gaia DR1 shows that stellar youth is only one of the reasons for field stars to have excess Nuv luminosities, and perhaps, not the main one. Dynamical and possibly magnetic interaction of low-mass dwarfs in close binaries is capable of supporting fast rotation rates and enhanced levels of X-ray and UV radiation for durations comparable to the main-sequence lifetimes. This is confirmed, for example, by in-depth investigations of stellar rotation rates in nearby open clusters. Douglas et al. (2016) find that almost all single members of the Hyades (age ≈ 650 Myr) with masses above $0.3\,M_\odot$ are slow rotators, while most of the spectroscopic binaries in this mass range are fast rotators. Many of the nearby stars listed in Table 1 with Nuv−G colors bluer than the main sequence are expected to be old binary systems of BY Dra type. In a wider sample of stars with extreme UV colors listed in Table 2, the presence of binaries with white dwarf and sdOB hot subdwarf components is conspicious, but many others remain hidden.

It is reasonable to expect that metal-poor Population II stars should also show mild Nuv excess compared with disk dwarfs. The weak absorption lines of metals in the near–UV region provide additional flux at short wavelengths. Since the fraction of Population II stars in the solar neighborhood is low, we expect few, if any, such objects to be present in our analysis. Using tangential velocities (computed from Gaia proper motions and parallaxes) as a proxy for population type, a search for high-velocity stars within 40 pc of the Sun resulted in 70 objects (out of 1403) with $v_{\mathrm{tan}} > 70$ km s^{-1}. These fast moving stars comply with the main sequence quite well (not shown in this paper for brevity) with the exception of a few objects deviating to the giant domain and possibly three stars with mild Nuv excess, all with Mnuv around 15 mag. Only one of the three objects satisfies the strict selection criteria adopted here, namely, the previously discussed spectroscopic

binary HIP 45731, but there is no evidence of metal deficiency in the literature.

It is also found that most of the field stars in the immediate solar neighborhood (distance less than 40 pc) follow a well-defined and narrow main sequence on the "absolute Nuv magnitude versus Nuv−G color" HR diagram constructed with Gaia parallaxes and GALEX and Gaia photometry. This confirms the high quality of GALEX and Gaia photometric data and makes such a diagram a valuable method to detect more stars with unusual UV radiation properties.

REFERENCES

Ansdell, M., Gaidos, E., Mann, A., et al. 2015, ApJ, 798, 41

Berger, J., & Fringant, A.-M. 1980, A&A, 85, 367

Bianchi, L., Herald, J., Efremova, B., et al. 2011, Ap&SS, 335, 161

Brown, A. G. A., and Gaia Collaboration. 2016, A&A, 595, A2

Chugainov, P. F. 1971, IBVS, 520, 1

Douglas, S. T., Agüeros, M. A., Covey, K. R., et al. 2016, ApJ, 822, 47

Eggelton, P.P., Kiseleva, L., Hut, P. 1998, ApJ, 499, 853

Elliott, P., Bayo, A., Melo, C. H. F., et al. 2016, A&A, 519, 13

ESA. 1997, The Hipparcos Catalogue, ESA SP-1200

Famaey, B., Pont, F., Luri, X., et al. 2007, A&A, 461, 957

Fontaine, G., Brassard, P., Bergeron, P., Wesemael, F. 1992, ApJ, 399, L91

Fuhrmann, K., Chini, R., Kaderhandt, L., Chen, Z., Lachaume, R. 2016, MNRAS, 459, 1682

Jancart, S., Jorissen, A., Babisiaux, C., Pourbaix, D. 2005, A&A, 442, 365

Gallagher, J. S., & Holm, A. V. 1974, ApJ, 189, 123

Gontcharov, G. A., Bajkova, A. T., Fedorov, P.N., Akhmetov, V. S. 2011, MNRAS, 413, 1581

Greenstein, J. L. 1974, ApJ, 189, L131

Herbig, G. H. & Moorhead, J. M. 1965, ApJ, 141, 649

Hernán-Obispo, M., Tuomi, M., Gálvez-Ortiz, M. C., et al. 2015, A&A, 576, 66

Høg, E., Fabricius, C., Makarov, V. V., et al. 2000, A&A, 357, 367

Hut, P. 1980, A&A, 92, 167

Kazarovets, E. V., Samus, N. N., Durlevich, O. V., Kireeva, N. N., Pastukhova, E. N. 2011, IBVS, 5969, 1

Kaitchuck, R. H., Mansperger, C. S., & Hantzios, P. A. 1988, ApJ, 330, 305

Khruslov, A. V. 2008, Peremennye Zvezdy Prilozhenie, 8, 4

Koen, C., & Eyer, L. 2002, MNRAS, 331, 45

Kraus, A. L., Shkolnik, E. L., Allers, K. N., Liu, M. C. 2014, AJ, 147, 146

Lépine, S., & Simon, M. 2009, AJ, 137, 3632

Lindegren, L., Lammers, U., Bastian, U., et al. 2016, A&A, 595, A4

Makarov, V. V. 2002, ApJ, 576, L61

————. 2003, AJ, 126, 1996

————. 2007, ApJS, 169, 105

Makarov, V. V., & Urban, S. 2000, MNRAS, 317, 289

Micela, G., Favata, F., & Sciortino, S. 1997, A&A, 326, 221

O'Donoghue, D., Kilkenny, D., Koen, C. 2013, MNRAS, 431, 240

Rodriguez, D., Zuckerman, B., Kastner, J. H., et al. 2013, ApJ, 774, 101

Samus', N. N., Goranskii, V. P., Durlevich, O. V., et al. 2003, Astronomy Letters, 29, 468

Shkolnik, E. L., Hebb, L., Liu, M. C., et al. 2010, ApJ, 716, 1522

Shkolnik, E. L., Anglada-Escudé, G., & Liu, M. 2012, ApJ, 758, 56

Shkolnik, E., Barman, T. S. 2014, AJ, 148, 64

Zasche, P., Svoboda, P., & Uhlar, R. 2012, A&A, 537, 109

Valeri V. Makarov: US Naval Observatory, 3450 Massachusetts Ave NW, Washington DC 20392-5420, USA (valeri.makarov@navy.mil).